

Warped Dynamic Linear Models for Time Series of Counts

Brian King and Daniel R. Kowal*
Department of Statistics, Rice University

Abstract

Dynamic Linear Models (DLMs) are commonly employed for time series analysis due to their versatile structure, simple recursive updating, and probabilistic forecasting. However, the options for count time series are limited: Gaussian DLMs require continuous data, while Poisson-based alternatives often lack sufficient modeling flexibility. We introduce a novel methodology for count time series by *warping* a Gaussian DLM. The warping function has two components: a transformation operator that provides distributional flexibility and a rounding operator that ensures the correct support for the discrete data-generating process. Importantly, we develop conjugate inference for the warped DLM, which enables analytic and recursive updates for the state space filtering and smoothing distributions. We leverage these results to produce customized and efficient computing strategies for inference and forecasting, including Monte Carlo simulation for offline analysis and an optimal particle filter for online inference. This framework unifies and extends a variety of discrete time series models and is valid for natural counts, rounded values, and multivariate observations. Simulation studies illustrate the excellent forecasting capabilities of the warped DLM. The proposed approach is applied to a multivariate time series of daily overdose counts and demonstrates both modeling and computational successes.

Keywords: Bayesian statistics; state-space model; particle filter; selection normal

*Brian King is PhD Student, Department of Statistics, Rice University, Houston, TX (bking@rice.edu). Daniel R. Kowal is Dobelman Family Assistant Professor, Department of Statistics, Rice University, Houston, TX (Daniel.Kowal@rice.edu). This material is based upon work supported by the National Science Foundation Graduate Research Fellowship under Grant No. 1842494.

1 Introduction

Count time series data inherit all the complexities of continuous time series data: the time-ordered observations may be multivariate, seasonal, dependent on exogenous variables, and exhibit a wide variety of autocorrelation structures. At the same time, count data often present uniquely challenging distributional features, including zero-inflation, over-/underdispersion, boundedness or censoring, and heaping. Additionally, discrete data require distinct strategies for probabilistic forecasting, uncertainty quantification, and evaluation. As modern datasets commonly feature higher resolutions and lengthier time series, computational tools for both online and offline inference and forecasting are in demand. Fundamentally, the goals in count time series modeling are similar to those in the continuous setting: forecasting, trend filtering/smoothing, seasonal decomposition, and characterization of inter- and intra-series dependence, among others.

In this paper, we develop methods, theory, and computing tools for a broad class of multivariate state-space models that address each of these challenges and objectives. The core model is defined by *warping* a Gaussian Dynamic Linear Model (DLM; [West and Harrison, 1997](#)):

$$\mathbf{y}_t = h(\mathbf{y}_t^*) \quad (\text{rounding}) \quad (1)$$

$$g(\mathbf{y}_t^*) = \mathbf{z}_t \quad (\text{transformation}) \quad (2)$$

$$\{\mathbf{z}_t\}_{t=1}^T \sim \text{DLM} \quad (\text{see (4) and (5)}) \quad (3)$$

where $\mathbf{y}_t \in \mathbb{N}^n$ is the observed count data and $\mathbf{z}_t \in \mathbb{R}^n$ is continuous latent data. Here, \mathbf{y}_t^* serves primarily as a explanatory bridge between model components, and in practice is not necessary to compute. The warping has two components: a rounding operator $h : \mathcal{T} \rightarrow \mathbb{N}^n$ in (1), which ensures the correct support for the discrete data-generating process, and a transformation function $g : \mathcal{T} \rightarrow \mathbb{R}^n$ in (2), which offers flexibility in the

marginal distributions. The rounding operator is particularly valuable for producing a coherent count-valued forecasting distribution and assists in modeling zero-inflated and bounded or censored data (see Section 2). By incorporating a latent DLM within the model, we enable straightforward embedding of familiar dynamic modeling structures such as local levels, seasonality, or covariates. Note that this article focuses on modeling counts, but the framework is easily adaptable for general integer-valued or rounded data.

The warped DLM (warpDLM) model (1)–(3) offers a unified framework for several (dynamic and non-dynamic) count data models. Among non-Bayesian methods, Siegfried and Hothorn (2020) demonstrated the benefits of learned transformations for discrete data linear regression, while Kowal and Wu (2021) adopted a related transformation and rounding strategy to model heaped count data. When $g(\cdot)$ is viewed as a copula, the warpDLM resembles the count time series model proposed by Jia et al. (2021). Unlike Jia et al. (2021), we do not focus on stationary latent Gaussian processes, but rather incorporate DLMs to enable nonstationary modeling, dynamic covariates, and Bayesian inference and forecasting within a familiar setting. Among Bayesian methods, Canale and Dunson (2011) and Canale and Dunson (2013) similarly applied rounded Gaussian and Dirichlet processes, respectively, without the transformation or dynamic considerations. Kowal and Canale (2020) demonstrated the benefits of both the rounding *and* transformation components within a (non-dynamic) regression setting. However, these Bayesian models did not derive closed-form posteriors and required MCMC-based approximations for posterior and predictive inference. A notable exception is Fasano et al. (2021) for dynamic probit models, but their approach only applies for binary data as a special case of the warpDLM.

A key contribution of this article is to develop conjugate inference for the warpDLM. In particular, we show that the warpDLM likelihood is conjugate to the *selection normal distribution* (e.g., Arellano-Valle et al., 2006). Based on this result, we derive analytic

and recursive updates for the state space filtering and smoothing distributions in (1)–(3). Crucially, we provide direct Monte Carlo simulators for these distributions—as well as the count-valued forecasting distribution—and construct an optimal particle filter for online inference. These models, derivations, and algorithms remain valid in the multivariate setting, and provide significant advancements over existing latent models for count time series (e.g., [Jia et al., 2021](#)).

The warpDLM framework belongs to the parameter-driven category of generalized state-space models ([Cox et al., 1981](#)). Parameter-driven models treat the latent state parameter as stochastic; they are often Bayesian or can be viewed as such, since model learning proceeds via recursive updating, for example using the Kalman filter ([Kalman, 1960](#)). The DLM is the most well-known model in this category, but it relies on Gaussian assumptions which are unmet by integer-valued data. Dynamic Generalized Linear Models (DGLMs) were developed to adapt the state-space framework for non-Gaussian data within the exponential family ([West et al., 1985](#)). For most count data, Poisson is the only available observational density that belongs to the exponential family. The negative binomial distribution with fixed dispersion parameter is also exponential family. However, there is often little guidance for determining the dispersion parameter, which is also incapable of modeling underdispersed count data. [Berry and West \(2019\)](#) recently extended the DGLM family by mixing Bernoulli and Poisson DGLMs to better model zero-inflated count data.

Although the Poisson DGLM and extensions are coherent for count time series data, the Kalman filtering results are generally unavailable. As a result, linearized approximations or MCMC algorithms are required for smoothing, filtering, and forecasting. One exception was introduced by [Gamerman et al. \(2013\)](#), who used a Poisson model with a multiplicative state update to preserve analytic and recursive inference. However, this updating structure has limited dynamic flexibility, for example to include seasonality or

covariates. [Aktekin et al. \(2018\)](#) proposed a multivariate extension of this multiplicative model, but the analytic updating results were not preserved and the multivariate structure only accommodated positive correlations among the series. Another exception is [Bradley et al. \(2018\)](#), who proposed log-Gamma processes that are conditionally conjugate to the Poisson distribution. However, their state space models still require Gibbs sampling for all state smoothing, filtering, and forecasting distributions. Poisson DGLMs more commonly incorporate Gaussian evolution equations (see (5)), but the filtering and smoothing distributions are not expressible in closed form, so approximations are required. [West et al. \(1985\)](#) defined conjugate priors for the natural parameter and approximated the filtering distribution in order to proceed with conjugate analysis. [Durbin and Koopman \(2000\)](#) used importance sampling based on a linear approximation.

The common limitations among existing state space models for count data are (i) the lack of analytic and recursive updates and (ii) the restricted options for count-valued distributions. The warpDLM framework directly addresses and overcomes both limitations.

The paper is organized as follows. Section 2 introduces DLMs, the proposed model, and examples for the rounding and transformation. In Section 3, we derive the smoothing, filtering, and forecasting distributions for the warpDLM. We discuss computing strategies for online and offline inference in Section 4. Finally, we present forecasting results on simulated data as well as a real-data application in Section 5 before concluding. Supplementary material includes proofs of presented theorems, discussion of Gibbs sampling for warpDLMs, and additional details on the real-data application model specification.

2 Dynamic Linear Models and Time Series of Counts

The broad success of Bayesian time series analysis has largely been driven by Dynamic Linear Models (DLMs), also known as linear state-space models. The DLM framework subsumes ARIMA models and provides decomposition of time series, dynamic regression analysis, and multivariate modeling capabilities. DLMs are widely popular not only because of their versatility, but also because the filtering, smoothing, and forecasting distributions are available in closed-form via the recursive Kalman filter.

A DLM is defined by two equations: (i) the observation equation, which specifies how the observations \mathbf{z}_t are related to the p -dimensional latent state vector $\boldsymbol{\theta}_t$ and (ii) the state evolution equation, which describes how the states are updated in a Markovian fashion. For an n -dimensional multivariate (continuous) time series $\{\mathbf{z}_t\}_{t=1}^T$, the (Gaussian) DLM is

$$\mathbf{z}_t = \mathbf{F}_t \boldsymbol{\theta}_t + \mathbf{v}_t, \quad \mathbf{v}_t \sim N_n(\mathbf{0}, \mathbf{V}_t) \quad (4)$$

$$\boldsymbol{\theta}_t = \mathbf{G}_t \boldsymbol{\theta}_{t-1} + \mathbf{w}_t, \quad \mathbf{w}_t \sim N_p(\mathbf{0}, \mathbf{W}_t) \quad (5)$$

for $t = 1, \dots, T$, where $\{\mathbf{v}_t, \mathbf{w}_t\}_{t=1}^T$ are mutually independent and $\boldsymbol{\theta}_0 \sim N_p(\mathbf{a}_0, \mathbf{R}_0)$. Depending on the DLM specification, the state vector $\boldsymbol{\theta}_t$ could describe a local level, regression coefficients, or seasonal components, among other features. The $n \times p$ observation matrix is \mathbf{F}_t , and is often the identity or the design matrix in a dynamic regression. The $p \times p$ state evolution matrix \mathbf{G}_t is frequently the identity but can be more complex, for example to capture seasonality. The observation and evolution covariance matrices are \mathbf{V}_t ($n \times n$) and \mathbf{W}_t ($p \times p$), respectively. Taken together, the quadruple $\{\mathbf{F}_t, \mathbf{G}_t, \mathbf{V}_t, \mathbf{W}_t\}_{t=1}^T$ defines the DLM. Often, these matrices will be time-invariant.

The Gaussian DLM (4)–(5) is incoherent and inadequate for count data. DGLMs are one attempt to adapt state-space models for counts, where the observation density is constrained to the exponential family. In contrast to this restrictive requirement, the

warpDLM framework (1)–(3) offers greater distributional flexibility via a transformation, but maintains the useful state-space formulation through the latent DLM. Furthermore, the rounding operator allows the warpDLM to model zero-inflated, over/underdispersed, or bounded/censored data (Kowal and Canale, 2020) and heaped data (Kowal and Wu, 2021). Notably, DGLMs cannot model these features without significant modifications. Additionally, by leveraging Gaussian state space models, we build on the long history of theoretical and computational tools (West and Harrison, 1997; Campagnoli et al., 2009; Prado and West, 2010), and operate within a familiar setting for practitioners.

The warpDLM framework links count data \mathbf{y}_t with a Gaussian DLM for \mathbf{z}_t in (4)–(5) by assuming that the data is a rounded version of some underlying continuous valued process \mathbf{y}_t^* with domain $\mathcal{T} \subseteq \mathbb{R}^n$. Specifically, the rounding operation $h : \mathcal{T} \rightarrow \mathbb{N}^n$ is a many-to-one function that inputs a set \mathcal{A}_j and outputs a vector of integers j ; when $n = 1$, \mathcal{A}_j is an interval and $j \in \mathbb{Z}$. Incorporating the transformation g , the warpDLM likelihood is

$$\mathbb{P}(\mathbf{y}_t = j | \boldsymbol{\theta}) = \mathbb{P}\{\mathbf{y}_t^* \in \mathcal{A}_j | \boldsymbol{\theta}\} = \mathbb{P}\{\mathbf{z}_t \in g(\mathcal{A}_j) | \boldsymbol{\theta}\}, \quad t = 1, \dots, T \quad (6)$$

for $j \in \mathbb{N}^n$, where $\mathbf{z}_t \in g(\mathcal{A}_j)$ is defined elementwise when \mathbf{y}_t is multivariate. As noted previously, \mathbf{y}_t^* helps clarify the model, but is unnecessary in implementation: the rounding and transformation steps can simply be chained into one warping operation $\mathbf{y}_t = h\{g^{-1}(\mathbf{z}_t)\}$.

Both components of the warping operation serve important purposes that lead directly to desirable model properties. The rounding function ensures that the warpDLM model has the correct support for the (possibly bounded or censored) count data. For simplicity, suppose $n = 1$; generalizations occur by applying these specifications elementwise. By default, we take the rounding function to be the floor function, so $\mathcal{A}_j = [j, j + 1)$. In addition, we include the zero modification $g(\mathcal{A}_0) = (-\infty, 0)$ so that $y_t = 0$ whenever $z_t < 0$. This specification maps much of the latent space to zero, with persistence of zeros

determined by the DLM (4)–(5), for example, $\mathbb{P}(y_t = 0 | y_{t-1} = 0) = \mathbb{P}(z_t < 0 | z_{t-1} < 0)$. Similarly, when there is a known upper bound y_{max} due to natural bounds or censoring, we may simply set $\mathcal{A}_{y_{max}} = [y_{max}, \infty)$ so that the warpDLM has the correct support, $\mathbb{P}(y_t \leq y_{max} | \boldsymbol{\theta}) = 1$. These useful rounding operation properties are formalized in [Kowal and Canale \(2020\)](#) and [Kowal and Wu \(2021\)](#). Importantly, the rounding operator does not require any modification to the computing algorithms: once it is specified, inference proceeds the exact same way for all choices of $h(\cdot)$.

Whereas the rounding operation allows us to model aspects of the data boundaries and ensures discreteness, the transformation function gives distributional flexibility for modeling the interior values. We apply the transformation elementwise, $g(\mathbf{y}_t^*) = (g_1(y_{1,t}^*), \dots, g_n(y_{n,t}^*))'$, and again present the case of $n = 1$ for simplicity. The only requirement of the transformation $g(\cdot)$ is that it be strictly monotonic, which preserves ordering in the latent data space and ensures an inverse exists. We can choose from well-known families of transformations, such as the (signed) Box-Cox ([Box and Cox, 1964](#)):

$$g(t; \lambda) = \{\text{sgn}(t)|t|^\lambda - 1\}/\lambda, \quad \lambda > 0 \tag{7}$$

with $g(t; \lambda = 0) = \log(t)$. Functions from this family have long been used to transform data towards normality, and thus represent a natural choice in the warpDLM context. [Kowal and Canale \(2020\)](#) employed this family of transformations for Bayesian regression modeling of non-dynamic count data. Alternatively, we can determine the transformation via a data-driven approach. [Kowal and Wu \(2021\)](#) proposed to determine g based on the marginal distribution of $\{y_t\}_{t=1}^T$. Specifically, let $\mathcal{A}_j = [a_j, a_{j+1})$ as above. Noting that the cumulative distribution function (CDF) of y and z are linked via $F_y(j) = F_z\{g(a_{j+1})\}$, [Kowal and Wu \(2021\)](#) suggested the transformation

$$\hat{g}_0(a_{j+1}) = \bar{y} + \hat{s}_y \Phi^{-1}\{\tilde{F}_y(j)\} \tag{8}$$

and then smoothly interpolated $(y_t, \hat{g}_0(a_{y_{t+1}}))$ using a monotonic spline, which ensures that the warpDLM is supported on \mathbb{N} instead of only the observed count values. This estimator matches the marginal moments of y_t and z_t , so \bar{y} and \hat{s}_y are the sample mean and sample standard deviation, respectively, of $\{y_t\}_{t=1}^T$. The transformation (8) allows flexibility in the estimator $\tilde{F}_y(j)$ of the marginal CDF of y : important examples include the nonparametric empirical CDF or parametric models such as Poisson or Negative Binomial marginals. Selection among transformations may proceed by examining model diagnostics or computing model comparison metrics, such as marginal likelihoods (see (16)).

3 Exact Filtering and Smoothing

In this section, we derive the analytic and recursive updates for the smoothing and filtering distributions of the warpDLM. These results are based on conjugacy properties with the selection normal distribution (Arellano-Valle et al., 2006), and crucially enable inference and forecasting without the use of MCMC.

3.1 Selection Distributions and the warpDLM

Consider the first time step $t = 1$ of the warpDLM. Here, we omit the time subscripts for simplicity. The latent data (3) are described by the two DLM equations (4)–(5), which can be rewritten as a single equation

$$\mathbf{z} = \mathbf{F}\boldsymbol{\theta} + \mathbf{v}, \quad \mathbf{v} \sim N_n(\mathbf{0}, \mathbf{V}) \quad (9)$$

with $\boldsymbol{\theta} := \boldsymbol{\theta}_1$ and the prior $\boldsymbol{\theta} \sim N_p(\boldsymbol{\mu}_\theta = \mathbf{G}a_0, \boldsymbol{\Sigma}_\theta = \mathbf{G}\mathbf{R}_0\mathbf{G}' + \mathbf{W})$. The posterior distribution in this case is the first-step filtering distribution, and can be written as

$$p(\boldsymbol{\theta}|\mathbf{y}) = p(\boldsymbol{\theta}|\mathbf{z} \in \mathcal{C}) = \frac{p(\boldsymbol{\theta})p\{\mathbf{z} \in \mathcal{C}|\boldsymbol{\theta}\}}{p\{\mathbf{z} \in \mathcal{C}\}} \quad (10)$$

where $\mathcal{C} = g(\mathcal{A}_y)$ is our constraint set. The filtering distribution conditions on \mathbf{y} , which in the warpDLM is equivalent to conditioning on \mathbf{z} belonging to some set. A random variable arising from this kind of conditioning is known as a selection distribution (Arellano-Valle et al., 2006). When the two variables are also jointly normal, as is the case with z and θ due to the DLM assumption, the resulting distribution is a *selection normal* (SLCT-N). More formally, given the joint distribution

$$\begin{pmatrix} z \\ \boldsymbol{\theta} \end{pmatrix} \sim N_{n+p} \left\{ \begin{pmatrix} \boldsymbol{\mu}_z \\ \boldsymbol{\mu}_\theta \end{pmatrix}, \begin{pmatrix} \boldsymbol{\Sigma}_z & \boldsymbol{\Sigma}_{z\theta} \\ \boldsymbol{\Sigma}'_{z\theta} & \boldsymbol{\Sigma}_\theta \end{pmatrix} \right\}$$

we denote the conditional random variable $[\boldsymbol{\theta} | \mathbf{z} \in \mathcal{C}] \sim \text{SLCT-N}_{n,p}(\boldsymbol{\mu}_z, \boldsymbol{\mu}_\theta, \boldsymbol{\Sigma}_z, \boldsymbol{\Sigma}_\theta, \boldsymbol{\Sigma}_{z\theta}, \mathcal{C})$ for constraint region \mathcal{C} . This random variable has density

$$p(\boldsymbol{\theta} | \mathbf{z} \in \mathcal{C}) = \phi_p(\boldsymbol{\theta}; \boldsymbol{\mu}_\theta, \boldsymbol{\Sigma}_\theta) \frac{\bar{\Phi}_n(\mathcal{C}; \boldsymbol{\Sigma}_{z\theta} \boldsymbol{\Sigma}_\theta^{-1} (\boldsymbol{\theta} - \boldsymbol{\mu}_\theta) + \boldsymbol{\mu}_z, \boldsymbol{\Sigma}_z - \boldsymbol{\Sigma}_{z\theta} \boldsymbol{\Sigma}_\theta^{-1} \boldsymbol{\Sigma}'_{z\theta})}{\bar{\Phi}_n(\mathcal{C}; \boldsymbol{\mu}_z, \boldsymbol{\Sigma}_z)} \quad (11)$$

where $\phi_p(\cdot; \boldsymbol{\mu}, \boldsymbol{\Sigma})$ denotes the Gaussian density function of a Gaussian random variable with mean $\boldsymbol{\mu}$ and covariance $\boldsymbol{\Sigma}$ and $\bar{\Phi}_n(\mathcal{C}; \boldsymbol{\mu}, \boldsymbol{\Sigma}) = \int_{\mathcal{C}} \phi_n(\mathbf{x}; \boldsymbol{\mu}, \boldsymbol{\Sigma}) d\mathbf{x}$. The density (11) is somewhat unwieldy in practice, but there is also a constructive representation which allows for direct Monte Carlo simulation from the posterior density $p(\boldsymbol{\theta} | \mathbf{y})$ (see Section 4).

For the first-step model (9) with prior $\boldsymbol{\theta} \sim N_p(\boldsymbol{\mu}_\theta, \boldsymbol{\Sigma}_\theta)$, we report the exact posterior distribution:

Theorem 1 (Kowal (2021)). *Under (9), the posterior distribution is $[\boldsymbol{\theta} | \mathbf{y}] \sim \text{SLCT-N}_{n,p}(\boldsymbol{\mu}_z = \mathbf{F}\boldsymbol{\mu}_\theta, \boldsymbol{\mu}_\theta, \boldsymbol{\Sigma}_z = \mathbf{F}\boldsymbol{\Sigma}_\theta\mathbf{F}' + \mathbf{V}, \boldsymbol{\Sigma}_\theta, \boldsymbol{\Sigma}_{z\theta} = \mathbf{F}\boldsymbol{\Sigma}_\theta, \mathcal{C} = g(\mathcal{A}_y))$.*

The Gaussian prior in Theorem 1 is conjugate: Gaussian distributions may be expressed as $[\boldsymbol{\theta}] \sim \text{SLCT-N}_{1,p}(\mu_z = 0, \boldsymbol{\mu}_\theta, \boldsymbol{\Sigma}_z = 1, \boldsymbol{\Sigma}_\theta, \boldsymbol{\Sigma}_{z\theta} = \mathbf{0}'_p, \mathcal{C} = \mathbb{R})$. The moments and constraints on \mathbf{z} are irrelevant as long as $\boldsymbol{\Sigma}_{z\theta} = \mathbf{0}$. However, the conjugacy suggests a more general prior for $\boldsymbol{\theta}$, namely, the SLCT-N distribution:

Lemma 1 (Kowal (2021)). Consider the prior $\boldsymbol{\theta} \sim \text{SLCT-N}_{n_0,p}(\boldsymbol{\mu}_{z_0}, \boldsymbol{\mu}_\theta, \boldsymbol{\Sigma}_{z_0}, \boldsymbol{\Sigma}_\theta, \boldsymbol{\Sigma}_{z_0\theta}, \mathcal{C}_0)$ with the latent observation equation (9). The posterior is

$$[\boldsymbol{\theta}|\mathbf{y}] \sim \text{SLCT-N}_{n_0+n,p} \left\{ \boldsymbol{\mu}_{z_1} = \begin{pmatrix} \boldsymbol{\mu}_{z_0} \\ \mathbf{F}\boldsymbol{\mu}_\theta \end{pmatrix}, \boldsymbol{\mu}_\theta, \boldsymbol{\Sigma}_{z_1} = \begin{pmatrix} \boldsymbol{\Sigma}_{z_0} & \boldsymbol{\Sigma}_{z_0\theta}\mathbf{F}' \\ \mathbf{F}\boldsymbol{\Sigma}'_{z_0\theta} & \mathbf{F}\boldsymbol{\Sigma}_\theta\mathbf{F}' + \mathbf{V} \end{pmatrix}, \boldsymbol{\Sigma}_\theta, \right. \\ \left. \boldsymbol{\Sigma}_{z_1\theta} = \begin{pmatrix} \boldsymbol{\Sigma}_{z_0\theta} \\ \mathbf{F}\boldsymbol{\Sigma}_\theta \end{pmatrix}, \mathcal{C}_1 = \mathcal{C}_0 \times g(\mathcal{A}_\mathbf{y}) \right\}.$$

Thus the selection normal distribution is conjugate with the warpDLM likelihood. Moreover, since the Gaussian distribution is closed under linear transformations, this property is preserved for the selection normal distribution (Arellano-Valle et al., 2006). These results link the selection normal distribution with the warpDLM prior-to-posterior updating mechanism, and provide the key building blocks for deriving the warpDLM filtering and smoothing distributions. These results are explored concurrently in Kowal (2021), which focuses on the (non-dynamic) linear regression (9) for discrete data.

3.2 Filtering and Smoothing for Warped DLMs

We now proceed to the most general setting for warpDLM, using the conjugacy and closure under linear transformation results to derive the exact forms of the filtering, smoothing, and forecasting distributions. Throughout, we assume the quadruple $\{\mathbf{F}_t, \mathbf{G}_t, \mathbf{V}_t, \mathbf{W}_t\}$ for each $t = 1, \dots, T$ is known. Estimation of the variance parameters is addressed in Section 4.

3.2.1 Filtering

Adding back the appropriate subscripts to Theorem 1, the first-step filtering distribution is $(\boldsymbol{\theta}_1|\mathbf{y}_1) \sim \text{SLCT-N}_{n,p}(\boldsymbol{\mu}_{z_1} = \mathbf{F}_1\mathbf{a}_1, \boldsymbol{\mu}_\theta = \mathbf{a}_1, \boldsymbol{\Sigma}_{z_1} = \mathbf{F}_1\mathbf{R}_1\mathbf{F}'_1 + \mathbf{V}_1, \boldsymbol{\Sigma}_\theta = \mathbf{R}_1, \boldsymbol{\Sigma}_{z_1\theta} =$

$\mathbf{F}_1 \mathbf{R}_1, \mathbf{C}_1 = g(\mathcal{A}_{\mathbf{y}_1})$, where $\mathbf{a}_1 = \mathbf{G}_1 \mathbf{a}_0$ and $\mathbf{R}_1 = \mathbf{G}_1 \mathbf{R}_0 \mathbf{G}'_1 + \mathbf{W}_1$. Given the first-step filtering distribution, we proceed inductively for time t :

Theorem 2. *Let*

$$(\boldsymbol{\theta}_{t-1} | \mathbf{y}_{1:t-1}) \sim SLCT-N_{n(t-1),p}(\boldsymbol{\mu}_{z_{t-1}|t-1}, \boldsymbol{\mu}_{\theta_{t-1}|t-1}, \boldsymbol{\Sigma}_{z_{t-1}|t-1}, \boldsymbol{\Sigma}_{\theta_{t-1}|t-1}, \boldsymbol{\Sigma}_{(z\theta)_{t-1}|t-1}, C_{t-1|t-1})$$

be the filtering distribution at time $t - 1$ under the warpDLM model. Then the one-step-ahead state predictive distribution at t is

$$(\boldsymbol{\theta}_t | \mathbf{y}_{1:t-1}) \sim SLCT-N_{n(t-1),p}(\boldsymbol{\mu}_{z_t|t-1}, \boldsymbol{\mu}_{\theta_t|t-1}, \boldsymbol{\Sigma}_{z_t|t-1}, \boldsymbol{\Sigma}_{\theta_t|t-1}, \boldsymbol{\Sigma}_{(z\theta)_t|t-1}, C_{t|t-1}) \quad (12)$$

with $\boldsymbol{\mu}_{z_t|t-1} = \boldsymbol{\mu}_{z_{t-1}|t-1}$, $\boldsymbol{\mu}_{\theta_t|t-1} = \mathbf{G}_t \boldsymbol{\mu}_{\theta_{t-1}|t-1}$, $\boldsymbol{\Sigma}_{z_t|t-1} = \boldsymbol{\Sigma}_{z_{t-1}|t-1}$, $\boldsymbol{\Sigma}_{\theta_t|t-1} = \mathbf{G}_t \boldsymbol{\Sigma}_{\theta_{t-1}|t-1} \mathbf{G}'_t + \mathbf{W}_t$, $\boldsymbol{\Sigma}_{(z\theta)_t|t-1} = \boldsymbol{\Sigma}_{(z\theta)_{t-1}|t-1} \mathbf{G}'_t$, and $C_{t|t-1} = C_{t-1|t-1}$. Furthermore, the filtering distribution at time t is

$$(\boldsymbol{\theta}_t | \mathbf{y}_{1:t}) \sim SLCT-N_{n(t),p}(\boldsymbol{\mu}_{z_t|t}, \boldsymbol{\mu}_{\theta_t|t}, \boldsymbol{\Sigma}_{z_t|t}, \boldsymbol{\Sigma}_{\theta_t|t}, \boldsymbol{\Sigma}_{(z\theta)_t|t}, C_{t|t}) \quad (13)$$

$$\text{with } \boldsymbol{\mu}_{z_t|t} = \begin{pmatrix} \boldsymbol{\mu}_{z_t|t-1} \\ \mathbf{F}_t \boldsymbol{\mu}_{\theta_t|t-1} \end{pmatrix}, \boldsymbol{\mu}_{\theta_t|t} = \boldsymbol{\mu}_{\theta_t|t-1}, \boldsymbol{\Sigma}_{z_t|t} = \begin{pmatrix} \boldsymbol{\Sigma}_{z_t|t-1} & \boldsymbol{\Sigma}_{(z\theta)_t|t-1} \mathbf{F}'_t \\ \mathbf{F}_t \boldsymbol{\Sigma}'_{(z\theta)_t|t-1} & \mathbf{F}_t \boldsymbol{\Sigma}_{\theta_t|t-1} \mathbf{F}'_t + \mathbf{V}_t \end{pmatrix}, \boldsymbol{\Sigma}_{\theta_t|t} = \boldsymbol{\Sigma}_{\theta_t|t-1}, \boldsymbol{\Sigma}_{(z\theta)_t|t} = \begin{pmatrix} \boldsymbol{\Sigma}_{(z\theta)_t|t-1} \\ \mathbf{F}_t \boldsymbol{\Sigma}_{\theta_t|t-1} \end{pmatrix}, \text{ and } C_{t|t} = C_{t|t-1} \times g(\mathcal{A}_{\mathbf{y}_t}).$$

The state predictive distribution updating in (12) is analogous to that of the Kalman filter, but the filtering distribution update in (13) has a different form. In the Kalman filter, one calculates the filtering distribution parameters by taking the previous best estimate for the states (from the state predictive distribution) and “correcting” them using information gained from the new observation. Under the warpDLM model, the previous parameters are not corrected; instead, the dimension of the new filtering distribution increases, with the information from the latest data point controlling the bounds over which the latent state

can vary. Importantly, the parameter updates depend on the new observation only through the selection region C , which implies that the system matrices do not need to be updated recursively. This point is better clarified by considering the smoothing distribution.

3.2.2 Smoothing

The joint smoothing distribution is $p(\boldsymbol{\theta}_{1:T}|\mathbf{y}_{1:T})$ where T is the terminal time point of our series. In the typical DLM setup, the filtering distribution parameters are first obtained in a recursive fashion, and then the smoothing parameters are determined by iterating back through the observations—the classic Forward Filter Backward Sampling (FFBS) algorithm (Carter and Kohn, 1994; Frühwirth-Schnatter, 1994). However, FFBS only gives the parameters of the marginal smoothing distributions, and it is nontrivial to construct the joint distribution within the framework of the Kalman filter.

In this regard, the warpDLM framework has an advantage: the joint smoothing distribution can be represented analytically. Furthermore, constructing the distribution does not require any passes through the data: instead, all smoothing parameters can be constructed *a priori* through relatively simple multiplications of the known matrices. The dependence on \mathbf{y}_t is solely through the constraint region.

The covariance matrix of $\boldsymbol{\theta}$ is the most complicated to construct. Let $\mathbf{G}_{1:t} = \mathbf{G}_t \cdot \mathbf{G}_{t-1} \cdots \mathbf{G}_1$ and $\boldsymbol{\mu}_\theta = (\mathbf{G}_{1:1}\mathbf{a}_0, \dots, \mathbf{G}_{1:T}\mathbf{a}_0)$, which is a $(p \cdot T) \times 1$ vector. Now, let $\mathbf{R}_t = \mathbf{G}_t \mathbf{R}_{t-1} \mathbf{G}'_t + \mathbf{W}_t$ for $t = 1, \dots, T$. Then the covariance matrix of $\boldsymbol{\theta}$ is defined as a $(p \cdot T) \times (p \cdot T)$ matrix with $p \times p$ diagonal block entries of $\boldsymbol{\Sigma}_\theta[t, t] = \mathbf{R}_t = \mathbf{G}_{1:t} \mathbf{R}_0 \mathbf{G}'_{1:t} + \sum_{q=2}^t \mathbf{G}_{q:t} \mathbf{W}_{q-1} \mathbf{G}'_{q:t} + \mathbf{W}_t$ and cross covariance entries (for $t > q$) $\boldsymbol{\Sigma}_\theta[t, q] = \boldsymbol{\Sigma}_\theta[q, t]^\top = \mathbf{G}_{(q+1):t} \boldsymbol{\Sigma}_\theta[q, q]$. We also define two block diagonal matrices, \mathfrak{F} and \mathfrak{V} , with diagonal entries of \mathbf{F}_t and \mathbf{V}_t , respectively, for $t = 1, \dots, n$, so \mathfrak{F} is a $nT \times pT$ matrix and \mathfrak{V} is a $nT \times nT$ matrix. Finally, let $\mathcal{C}_{1:T} = (g(\mathcal{A}_{y_1}), \dots, g(\mathcal{A}_{y_T}))$ be the vector of selection intervals through

time T . The joint smoothing distribution is given below:

Theorem 3. *Under the warpDLM model, the joint smoothing distribution is*

$$(\boldsymbol{\theta}_{1:T}|\mathbf{y}_{1:T}) \sim SLCT-N_{nT,pT}\{\boldsymbol{\mu}_z=\boldsymbol{\mathfrak{F}}\boldsymbol{\mu}_\theta, \boldsymbol{\mu}_\theta, \boldsymbol{\Sigma}_z=\boldsymbol{\mathfrak{V}} + \boldsymbol{\mathfrak{F}}\boldsymbol{\Sigma}_\theta\boldsymbol{\mathfrak{F}}', \boldsymbol{\Sigma}_\theta, \boldsymbol{\Sigma}_{z\theta}=\boldsymbol{\mathfrak{F}}\boldsymbol{\Sigma}_\theta, \mathcal{C}=\mathcal{C}_{1:T}\} \quad (14)$$

We can also adapt the notation from the smoothing setting to write out the time s filtering distribution parameters $p(\boldsymbol{\theta}_{1:s}|\mathbf{y}_{1:s})$ in a more straightforward manner. In particular, if we let the smoothing notation above be defined analogously, but only up to time point s instead of the terminal time point T , we can rewrite the parameters of the filtering distribution as $\boldsymbol{\mu}_{z_{s|s}} = \boldsymbol{\mathfrak{F}}\boldsymbol{\mu}_\theta$, $\boldsymbol{\mu}_{\theta_{s|s}} = \mathbf{G}_1^s \mathbf{a}_0$, $\boldsymbol{\Sigma}_{z_{s|s}} = \boldsymbol{\mathfrak{V}} + \boldsymbol{\mathfrak{F}}\boldsymbol{\Sigma}_\theta\boldsymbol{\mathfrak{F}}'$, $\boldsymbol{\Sigma}_{(z\theta)_{s|s}} = \boldsymbol{\mathfrak{F}}\boldsymbol{\Sigma}_\theta$, $\boldsymbol{\Sigma}_{\theta_{s|s}} = \mathbf{R}_s$. Although these covariance terms are quite complex in terms of notation, constructing such matrices is computationally straightforward via matrix multiplications and additions.

The marginal smoothing distribution $p(\boldsymbol{\theta}_t|\mathbf{y}_{1:T})$ at each time t is readily available from Theorem 3. In particular, the SLCT-N family is closed under marginalization, so the parameters for the observations stay the same as in the joint case, and we simply pick off the correct block of the state parameters. This is formalized in the corollary below.

Corollary 1. *Under the warpDLM model, the marginal smoothing distribution at time t is*

$$\begin{aligned} (\boldsymbol{\theta}_t|\mathbf{y}_{1:T}) \sim SLCT-N_{nT,p}\{\boldsymbol{\mu}_{z_t|T} = \boldsymbol{\mathfrak{F}}\boldsymbol{\mu}_\theta, \boldsymbol{\mu}_{\theta_t|T} = \boldsymbol{\mu}_\theta[t], \boldsymbol{\Sigma}_{z_t|T} = \boldsymbol{\mathfrak{V}} + \boldsymbol{\mathfrak{F}}\boldsymbol{\Sigma}_\theta\boldsymbol{\mathfrak{F}}', \boldsymbol{\Sigma}_{\theta_t|T} = \boldsymbol{\Sigma}_\theta[t, t], \\ \boldsymbol{\Sigma}_{(z\theta)_t|T} = \boldsymbol{\Sigma}_{z\theta}[, t], \mathcal{C} = \mathcal{C}_{1:T}\}. \end{aligned} \quad (15)$$

where $\boldsymbol{\Sigma}_{z\theta}[, t]$ refers to the t -th block of p columns in $\boldsymbol{\Sigma}_{z\theta}$.

Compared to the joint smoothing distribution in (14), the parameters of the marginal smoothing distribution in (15) have lower dimension. In particular, sampling from (15) requires drawing from a p -variate normal distribution, as opposed to a pT -variate normal for the joint distribution, but both require sampling from an nT -variate truncated normal;

see Section 4.1. In practice, the dimension of the truncated normal is the more limiting, and consequently it is often preferable to sample from the joint over the marginal distributions.

The joint smoothing distribution also enables direct computation of the warpDLM marginal likelihood:

Corollary 2. *Under the warpDLM model, the marginal likelihood is*

$$p(\mathbf{y}_{1:T}) = \bar{\Phi}_{nT}(\mathcal{C}_{1:T}; \boldsymbol{\mu}_z = \mathfrak{F}\boldsymbol{\mu}_\theta, \boldsymbol{\Sigma}_z = \mathfrak{V} + \mathfrak{F}\boldsymbol{\Sigma}_\theta\mathfrak{F}') . \quad (16)$$

The marginal likelihood is useful for marginal maximum likelihood estimation of the variance parameters in (4)–(5) and other model comparison metrics, for example to select the transformation g .

3.2.3 Forecasting

Filtering and smoothing allow us to retrospectively model the observed data, but often we are most interested in predicting the future counts, i.e. forecasting. Just as the marginal likelihood is the normalizing constant of the smoothing distribution, $p(\mathbf{y}_{1:(t+1)})$ is the normalizing constant of the filtering distribution at time $t+1$. Let $\boldsymbol{\mu}_{z_{t+1}|t+1}$ and $\boldsymbol{\Sigma}_{z_{t+1}|t+1}$ be the corresponding parameters of this distribution and $\mathcal{C}_{1:t}$ be the vector of selection intervals up to the known time t . Then the one step forecasting distribution is

$$p(\mathbf{y}_{t+1}|\mathbf{y}_{1:t}) = \frac{p(\mathbf{y}_{1:(t+1)})}{p(\mathbf{y}_{1:t})} = \frac{\bar{\Phi}_{n(t+1)}\{\mathcal{C}_{1:t} \times g(\mathcal{A}_{y_{t+1}}); \boldsymbol{\mu}_{z_{t+1}|t+1}, \boldsymbol{\Sigma}_{z_{t+1}|t+1}\}}{\bar{\Phi}_{nt}(\mathcal{C}_{1:t}; \boldsymbol{\mu}_{z_t}, \boldsymbol{\Sigma}_{z_t})} . \quad (17)$$

The h -step ahead forecasting distribution can be defined similarly. In most applications, the forecasting distribution is defined over all non-negative integers, and thus evaluating it for every point is not possible. However, in practice most time series of counts take values in a small range (especially locally), and thus the forecasting distribution will only put

significant mass on a small range of values. For short to medium time series applications, evaluating these probabilities is quite fast and does not pose a computational burden.

More directly, it is straightforward to simulate from the forecasting distribution given draws from the filtering distribution. Specifically, let $\boldsymbol{\theta}_t^* \sim (\boldsymbol{\theta}_t | \mathbf{y}_{1:t})$ denote a draw from the filtering distribution. By passing this draw through the DLM, the evolution equation (5) samples $\boldsymbol{\theta}_{t+1}^{**} \sim N_p(\mathbf{G}_{t+1}\boldsymbol{\theta}_t^*, \mathbf{W}_{t+1})$ and the observation equation (4) samples $\mathbf{z}_{t+1}^* \sim N_n(\mathbf{F}_t\boldsymbol{\theta}_{t+1}^{**}, \mathbf{V}_{t+1})$, which equivalently yields a draw from $(\mathbf{z}_{t+1} | \mathbf{y}_{1:t})$. By retaining $\tilde{\mathbf{y}}_{t+1} = h\{g^{-1}(\mathbf{z}_{t+1}^*)\}$, we obtain a draw from the one-step forecasting distribution of the warpDLM; multi-step forecasting proceeds similarly. Hence, the primary computational cost is the draw from the filtering distribution, which is detailed in Section 4.

4 Computing

We develop multiple computing strategies for both offline and online inference and forecasting. For offline inference, we propose direct Monte Carlo sampling from the relevant filtering or smoothing distributions. Notably, this strategy avoids the need for MCMC, which often requires lengthy simulation runs and various diagnostics. Online inference is enabled by an optimal particle filter. These two computing strategies—direct Monte Carlo sampling and optimal particle filtering—are uniquely available as a consequence of the results in Section 3. Lastly, the supplementary material provides an alternative offline algorithm via Gibbs sampling, which can decrease raw computing time at the expense of sampling efficiency when T is large.

4.1 Direct Sampling

Analytic filtering and smoothing distributions for the warpDLM unlock the possibility of direct Monte Carlo sampling, but this requires being able to efficiently sample from the selection normal. As noted in Section 3.1 and proved in Arellano-Valle et al. (2006), the SLCT-N can be represented constructively using draws from a multivariate normal distribution and a multivariate truncated normal distribution. Algorithm 1 details the process for one draw from a general selection normal distribution.

Algorithm 1: Sampling from Selection Normal Distribution

Result: One sample $\boldsymbol{\theta}$ from SLCT-N distribution

Given $[\boldsymbol{\theta}] \sim \text{SLCT-N}_{d_1, d_2}(\boldsymbol{\mu}_z, \boldsymbol{\mu}_\theta, \boldsymbol{\Sigma}_z, \boldsymbol{\Sigma}_\theta, \boldsymbol{\Sigma}_{z\theta}, \mathcal{C})$;

1. **Sample from truncated multivariate normal:** Sample \mathbf{V}_0 from $N_{d_1}(\mathbf{0}, \boldsymbol{\Sigma}_z)$ truncated to region $\mathcal{C} - \boldsymbol{\mu}_z$
 2. **Sample from multivariate normal:** Sample \mathbf{V}_1 from $N_{d_2}(\mathbf{0}, \boldsymbol{\Sigma}_\theta - \boldsymbol{\Sigma}'_{z\theta} \boldsymbol{\Sigma}_z^{-1} \boldsymbol{\Sigma}_{z\theta})$
 3. **Combine results:** Compute $\boldsymbol{\theta} = \boldsymbol{\mu}_\theta + \mathbf{V}_1 + \boldsymbol{\Sigma}'_{z\theta} \boldsymbol{\Sigma}_z^{-1} \mathbf{V}_0$
-

We can use this algorithm to directly sample from the warpDLM state predictive distribution (12), filtering distribution (13), joint smoothing distribution (14), or marginal smoothing distribution (15). It must be noted that direct sampling requires us to have already estimated our variance parameters \mathbf{V}_t and \mathbf{W}_t , for example using marginal likelihood in an empirical Bayes analysis.

The most computationally burdensome part of obtaining a Monte Carlo draw is sampling from the multivariate truncated normal. Several methods have been proposed to sample from such a distribution, and recently Botev (2017) introduced a state-of-the-art

procedure based on minimax tilting, implemented in the R package `TruncatedNormal`. This method is highly efficient and accurate for dimensions up to about $nT \approx 500$.

4.2 Optimal Particle Filtering

To circumvent the computational limitations of direct sampling (Section 4.1), we design an optimal particle filter that does not depend on the time dimension, thus enabling us to draw from the filtering distribution in such a setting. Within the state space literature, online particle filtering methods are usually Sequential Importance Sampling (SIS) or SIS with Resampling algorithms (Doucet et al., 2000). For each time point, sample trajectories or particles are drawn from an importance function, and each particle has an associated importance weight. With the resampling step, draws from the filtering distribution are obtained via a weighted resampling from the previously drawn particles. The purpose of this resampling step is to slow the effect of particle degeneration. A well-known drawback of particle filtering methods is that the variance of the importance weights grows over time, and thus the trajectories will degenerate, eventually leaving only one particle with nonzero weight. To avoid quick degeneration, it is important to choose a good importance function, and the optimal function is that which minimizes the variance of weights. Adapting the results of Doucet et al. (2000) to the notation of our warpDLM framework, this optimal importance function is $p(\boldsymbol{\theta}_t | \boldsymbol{\theta}_{t-1}, \mathbf{y}_t)$ with weights given by $p(\mathbf{y}_t | \boldsymbol{\theta}_{t-1})$. For many state space models, this function is not known analytically, but the selection normal theory from Section 3 gives us an exact form under the warpDLM framework, formalized in the following corollary.

Corollary 3. *Under the warpDLM model, we have*

$$\begin{aligned} (\boldsymbol{\theta}_t | \boldsymbol{\theta}_{t-1}, \mathbf{y}_t) &\sim \text{SLCT-}N_{n,p}(\boldsymbol{\mu}_z = \mathbf{F}_t \mathbf{G}_t \boldsymbol{\theta}_{t-1}, \boldsymbol{\mu}_\theta = \mathbf{G}_t \boldsymbol{\theta}_{t-1}, \boldsymbol{\Sigma}_z = \mathbf{V}_t + \mathbf{F}_t \mathbf{W}_t \mathbf{F}_t', \\ &\boldsymbol{\Sigma}_\theta = \mathbf{W}_t, \boldsymbol{\Sigma}_{z\theta} = \mathbf{F}_t \mathbf{W}_t, C = g(\mathcal{A}_{\mathbf{y}_t})) \end{aligned} \quad (18)$$

and

$$p(\mathbf{y}_t | \boldsymbol{\theta}_{t-1}) = \bar{\Phi}_n(g(\mathcal{A}_{\mathbf{y}_t}); \boldsymbol{\mu}_z = \mathbf{F}_t \mathbf{G}_t \boldsymbol{\theta}_{t-1}, \boldsymbol{\Sigma}_z = \mathbf{V}_t + \mathbf{F}_t \mathbf{W}_t \mathbf{F}_t') \quad (19)$$

With this in mind, we can construct our particle filter, given in Algorithm 2. The particle filter presented in Fasano et al. (2021) is a special case for probit DLMs. Notice that drawing from the selection normal in (18) is not dependent on the length of the time series, and thus we will not run into the computational problems of direct sampling.

Algorithm 2: Optimal Particle Filter for Warped DLM

Result: Draws $(\boldsymbol{\theta}_t^{(1)}, \dots, \boldsymbol{\theta}_t^{(S)})$ from filtering distribution $p(\boldsymbol{\theta}_t | \mathbf{y}_{1:t})$ for $t = 1, \dots, T$
 Given S particle trajectories at time $t = 0$ denoted by $\boldsymbol{\theta}_0^{(s)}$;

for $t \leftarrow 1$ **to** T **do**

for $s \leftarrow 1$ **to** S **do**

 Sample $\tilde{\boldsymbol{\theta}}_t^{(s)}$ from (18) conditional on $\boldsymbol{\theta}_{t-1} = \boldsymbol{\theta}_{t-1}^{(s)}$;

 Calculate weight up to normalizing constant using (19): $w_t^{(s)} \propto p(\mathbf{y}_t | \boldsymbol{\theta}_{t-1}^{(s)})$

end

 Normalize importance weights: $\tilde{w}_t^{(s)} = \frac{w_t^{(s)}}{\sum_{s=1}^S w_t^{(s)}}$;

 Obtain final draws $\boldsymbol{\theta}_t^{(1)}, \dots, \boldsymbol{\theta}_t^{(S)}$ by resampling $\tilde{\boldsymbol{\theta}}_t^{(1)}, \dots, \tilde{\boldsymbol{\theta}}_t^{(S)}$ with weights $\tilde{w}_t^{(s)}$

end

Particle filtering algorithms output weighted samples, and thus any summarization must take into account these weights. Here we resample at every time step, which gives equally weighted draws but also can decrease the diversity of the sampled state trajectories.

Future research could look at the effect on algorithm performance of different schemes, e.g., stratified sampling or residual resampling.

The (unnormalized) weights can also be used to compute an estimate of the marginal likelihood $p(\mathbf{y}_{1:T})$. Namely, we define

$$\hat{p}(\mathbf{y}_{1:T}) := \hat{p}(\mathbf{y}_1) \prod_{t=2}^T \hat{p}(\mathbf{y}_t | \mathbf{y}_{1:t-1}) \quad (20)$$

where $\hat{p}(\mathbf{y}_1) = \frac{1}{S} \sum_{s=1}^S w_1^{(s)}$ and $\hat{p}(\mathbf{y}_t | \mathbf{y}_{1:t-1}) = \frac{1}{S} \sum_{s=1}^S w_t^{(s)}$. As with equation (16), this can be used for model comparisons or estimation of unknown parameters (Kantas et al., 2015). Such an approximation is also key when designing more complex sequential Monte Carlo schemes or sampling based on particle methods (Andrieu et al., 2010).

Particle filtering is not necessarily a direct competitor with other methods of sampling. Instead, an offline analysis is often run (using either direct Monte Carlo or Gibbs sampling), and then the resulting parameter estimates and sampled states are used to initialize the particle filter. We show an example of this kind of tandem analysis in Section 5.3.

5 Warped DLMS in Action

In this section, we showcase several facets of the warpDLM framework. We first perform a forecasting analysis on simulated data, showing that the warpDLM offers better distributional forecasting than comparable Bayesian methods. Then we look at a real data application, namely counts of drug overdose reports in Cincinnati, and explore how we can use Gibbs sampling alongside the particle filter in a multivariate setting. Before delving into the analyses, we briefly discuss evaluation of distributional forecasts for discrete data.

5.1 Evaluating Probabilistic Forecasts

An advantage of the warpDLM method is that it provides “data coherent” forecasts (Free-land and McCabe, 2004), in the sense that it gives predictions appropriate to the type of data (counts in this case). Furthermore, the Bayesian nature of the framework gives access to the entire forecasting distribution. In general, point forecasts are not very informative in the discrete setting, and focus should typically be placed on evaluating the predictive distribution as a whole (Kolassa, 2016). Evaluation of probabilistic forecasts should first and foremost verify that forecast distributions are *calibrated* in the sense that the observed values are consistent with samples from the distribution (Czado et al., 2009). A commonly used diagnostic for calibration is the randomized Probability Integral Transform (rPIT). In particular, we assume there is some true (discrete) cumulative forecasting distribution H_t , from which a count y_t is observed. Each model produces an estimate \hat{H}_t of the forecasting distribution. The randomized PIT value is drawn from

$$\tilde{p}_t \stackrel{iid}{\sim} \text{Uniform}[\hat{H}_t(y_t - 1), \hat{H}_t(y_t)] . \quad (21)$$

If the model is well-calibrated, then $\hat{H}_t = H_t$ and consequently $\tilde{p}_t \stackrel{iid}{\sim} \text{Uniform}(0, 1)$. Thus, forecasts across multiple times t are evaluated by drawing (21) for each time point and comparing them to a standard uniform distribution.

Among calibrated forecasts, we then look to the *sharpness* of the forecasting distribution, such as the tightness of the prediction intervals. Czado et al. (2009) propose to evaluate the sharpness via scoring rules, in particular the logarithmic scoring rule $-\log(p_x)$ where p_x is the probability mass of the predictive distribution at the observed count x . We will utilize these diagnostics and measures to evaluate various warpDLM models and DGLM competitors in the following sections.

5.2 Forecasting on Simulated Data

Existing models for count time series are often unable to capture multiple challenging discrete distributional features, such as zero-inflation, boundedness, and heaping. In this setting, the warpDLM provides a natural and robust alternative. At the same time, the warpDLM is sufficiently flexible to model simpler count data settings for which existing models have been designed, such as Poisson data. To showcase this breadth of modeling, we designed simulation experiments to replicate both of these scenarios, and then tested the forecasting performance of various warpDLM models against their Bayesian peers (namely, DGLMs).

In the first experiment, we simulated zero-inflated and bounded count time series data. One real-world example of such data is analyzed in [Ensor et al. \(2014\)](#), where the quantity of interest is the number of hours per day which exceed a certain pollutant threshold. Many days show no pollution, leading to zero inflation, but occasionally every hour in a day exceeds the threshold, which result in bounded values of 24. Specifically, we sampled from a zero-inflated Poisson with time varying mean λ_t , where $\lambda_1 \sim \text{Uniform}(5, 15)$ and $\lambda_{t+1} \sim N(\lambda_t, .2)$ for $t = 2, \dots, T$. The zero-inflation component was drawn randomly from the interval .1 to .3. Any sampled value above 24 was rounded down to the bound.

In the second scenario, we simulated data from the INGARCH class using the R package `tscount` ([Liboschik et al., 2017](#)). An INGARCH(p, q) model assumes $y_t \sim \text{Poisson}(\lambda_t)$ with

$$\lambda_t = \beta_0 + \sum_{k=1}^p \beta_k Y_{t-k} + \sum_{\ell=1}^q \alpha_\ell \lambda_{t-\ell}. \quad (22)$$

Note that there are various stationarity constraints on the β s and the α s which limit the values that can be taken (see [Fokianos et al. \(2009\)](#) for more details). In our simulation, we chose relatively simple dynamics of $p = 1$ and $q = 1$ and set $\beta_0 = .3$, $\beta_1 = .6$, and $\beta_2 = .2$, with coefficient values selected such that simulated series were low-count time series.

For both DGPs, 30 time series of length $T = 200$ were simulated. We chose three different models from our warpDLM class to evaluate, each with the same latent local level DLM, but different transformations: the Box-Cox transformation (7) with identity ($\lambda = 1$) or square root ($\lambda = 1/2$) specifications and the nonparametric CDF (8). A local level DLM has a univariate state θ_t and is defined by the time-invariant system $\{1, 1, V, W\}$, with the initial state θ_0 given a $N(0, 3)$ prior. V and W were estimated via maximization of the marginal likelihood (16) and then Monte Carlo samples from the joint smoothing distribution (14) were drawn using Algorithm 1. These draws were used to simulate from the forecasting distribution, as outlined in Section 3.2.3.

For comparison, we considered both Poisson and negative binomial DGLMs with similar random walk dynamics for the state, with variances determined via maximum likelihood estimation. For the negative binomial DGLM, we used the default value of the dispersion parameter in KFAS. It is worth noting that it took several tries to find an initial value which resulted in convergence for the maximum likelihood estimation of the parameters for the DGLM models. In general, the likelihoods of state space models often have complex landscapes which can make parameter estimation difficult and sensitive to starting inputs (Helske, 2017). For the warpDLM methods, a suitable starting point was found by running a Gibbs sampler for a short number of iterations and using the posterior means as the input to the optimization algorithm.

In order to evaluate the forecasting performances, we used time series cross-validation for one-step-ahead predictions. Starting at $t = 100$, each of the five methodologies (three warpDLM methods and two DGLM methods) were fitted and one-step-ahead forecasts were drawn. For 50 equally dispersed time points from $t = 100$ to $t = 200$, the process of training and drawing one-step ahead forecasts was repeated. Thus, we have 50 observations to compare to 50 one-step-ahead forecasts for each of the 30 time series.

Since we are evaluating a multitude of series, we follow [Kolassa \(2016\)](#) in testing the uniformity of the rPIT values using the data-driven smooth test of [Ledwina \(1994\)](#). Hence, the output is a p-value, where smaller values indicate poor calibration. We then consider the sharpness by evaluating the logarithmic scoring rule. Our output for these models is 5000 draws from the predictive distribution, so we approximate the probability mass by calculating the proportion of draws which predicted that value. If a value was not sampled in any of the posterior draws, but was observed, then the logarithmic scoring rule would be infinite. To avoid this, we instead set the mass in that case to 0.0001. For each time series, we find the mean log score across the 50 time points and then compute the percent difference over a baseline method, chosen to be the Poisson DGLM. The logarithmic scoring rule is negatively oriented, so a negative percent difference equates to improved forecasting.

Figure 1 showcases calibration and sharpness results across simulations for the zero-inflated Poisson example. A clear takeaway is that the warpDLM model with nonparametric CDF transformation is well-calibrated, with the identity warpDLM also showing indications of uniformity in many of the simulations, showing that the rounding operation is a key component in proper forecasts. However, the rest of the models produce very low p-values for almost every simulation, indicating the rPIT scores are not uniform and therefore the models are not well-calibrated. Under the paradigm of [Czado et al. \(2009\)](#), such poor calibration should automatically lead us to disregard such models. If we then look at sharpness via the log score, the same picture emerges: the CDF-based transformation leads to the best distributional forecasts (on average 30% better than Poisson DGLM), with the identity transformation as the second best. Thus, with both good calibration and maximal sharpness, it is quite clear that the warpDLM framework can provide significant forecasting gains in this context.

The first simulation represents a situation where the warpDLM outshines all other

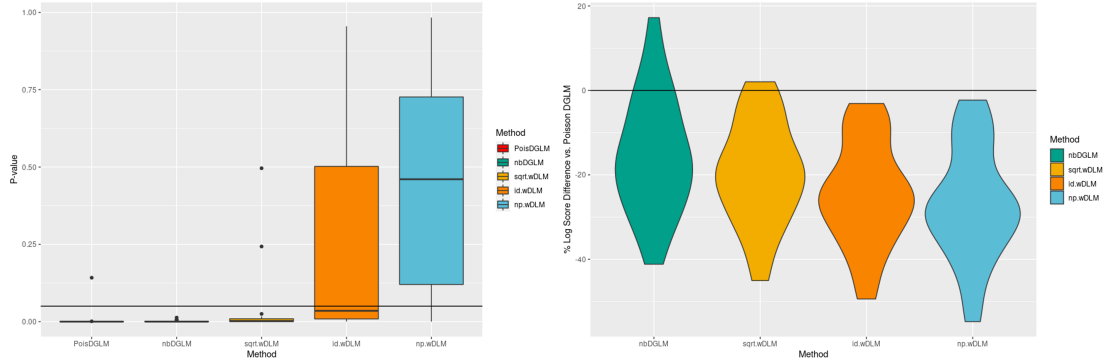


Figure 1: Zero-inflated Poisson simulations; Left: p-values resulting from test of uniformity across simulations, with line drawn at $p=0.05$; Right: % differences of log score compared to baseline (negative difference implies improved forecasting relative to Poisson DGLM)

methods. In the second simulation, we create data that should be well modeled by the Poisson DGLM. In this case, though, we see the warpDLM has the flexibility to match, and in some cases improve upon, the DGLM forecasting. Figure 2 shows the calibration and sharpness for the INGARCH simulations. All five models show proper calibration for almost all series. Furthermore, the three warpDLM models all show sharpness similar to the Poisson DGLM, and the warpDLM with square root transformation actually appears to improve on the forecasting for the majority of the series. The negative binomial DGLM performs uniformly worse than the Poisson DGLM.

5.3 Real Data Analysis

The results of the previous section show that the warpDLM framework is capable of modeling multiple data-generating processes and improves over competing methods in terms of forecasting performance. In this section, we use a real-world dataset to illustrate how the warpDLM can handle multivariate time series, which is a challenge for most count time

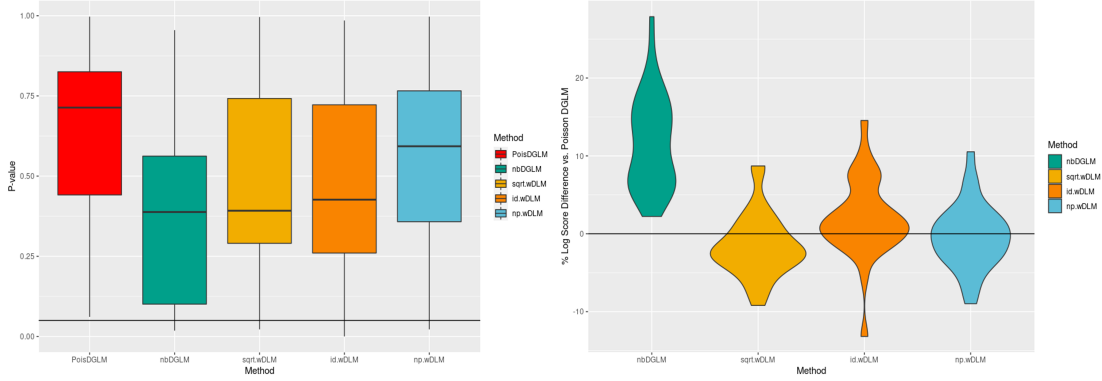


Figure 2: INGARCH simulations; Left: p-values resulting from test of uniformity across simulations, with line drawn at $p=0.05$; Right: % differences of log score compared to baseline (negative difference implies improved forecasting relative to Poisson DGLM)

series models. Furthermore, we display the adaptability of computation for warpDLM models, demonstrating how analysts can perform both offline and online inference.

We analyze the daily counts of drug overdose reports in Cincinnati, separated into two categories: heroin and non-heroin ($n = 2$). Cincinnati has dealt with a severe problem with drug overdoses in the city, and in particular heroin (Li et al., 2019). The overdose reports data are contained within a dataset of all fire and EMS incidents, available from the [city’s open access data repository](#). The data wrangling and cleaning process is described in the supplement. This bivariate count time series spans January 1st, 2018 to January 31st, 2021. We split these dates further into two time periods, performing an offline analysis for the years of 2018 and 2019, then switching to an online particle filter for the 2020 and January 2021 data. Thus we have $T = 730$ for the offline method and $T = 397$ for the sequential MCMC. Figure 3 shows the two time series for the full period. Overlaid on the series are the pointwise medians of draws from the smoothing predictive distribution $p(\tilde{\mathbf{y}}_{1:T}|\mathbf{y}_{1:T})$ from the warpDLM. Specifically, we take each sampled path of states $\boldsymbol{\theta}_{1:T}^* \sim p(\boldsymbol{\theta}_{1:T}|\mathbf{y}_{1:T})$,

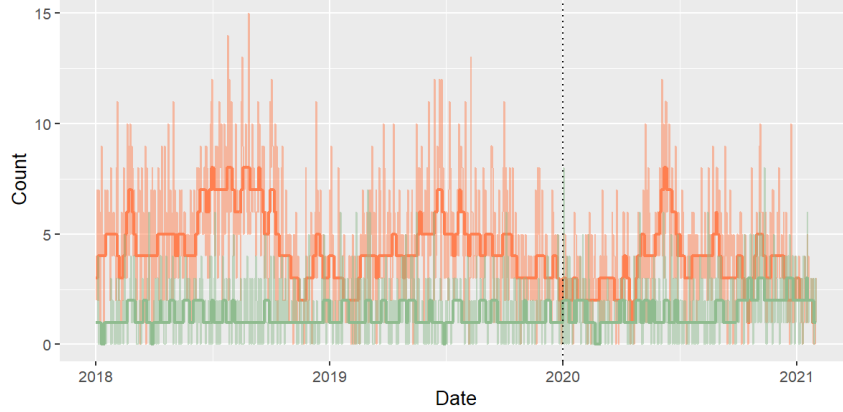


Figure 3: A plot of the two time series—the series with greater values is EMS calls for heroin ODs, and the lower one is all other OD calls. The dotted vertical line represents the transition between the online and offline datasets. The bolded lines overlaid on each series are median smoothed predictions of the data from the model output.

then draw a corresponding path $\tilde{\mathbf{z}}_{1:T}$ via the DLM observation equation (4), and finally set $\tilde{\mathbf{y}}_{1:T} = h\{g^{-1}(\tilde{\mathbf{z}}_{1:T})\}$, similar to the forecasting procedure in Section 3.2.3. By computing the median of this predictive distribution, we obtain a count-valued point estimate that “smooths” each time series conditional on the complete data $\mathbf{y}_{1:T}$.

The warpDLM features a linear growth model for each series $i \in \{1, 2\}$:

$$z_{i,t} = \mu_{i,t} + v_{i,t} \quad (23)$$

$$\mu_{i,t} = \mu_{i,t-1} + \beta_{i,t-1} + w_{i,t-1}^\mu \quad (24)$$

$$\beta_{i,t} = \beta_{i,t-1} + w_{i,t-1}^\beta \quad (25)$$

where $\mu_{i,t}$ is a local level, $\beta_{i,t}$ is a slope, and (24)–(25) comprise the DLM evolution equation (5). Dependence between the $n = 2$ series is induced by the observation error distribution $\mathbf{v}_t \sim N_2(\mathbf{0}, \mathbf{V})$ and the state error distributions $\mathbf{w}_t^\mu \sim N_2(\mathbf{0}, \mathbf{W}_\mu)$ and $\mathbf{w}_t^\beta \sim N_2(\mathbf{0}, \mathbf{W}_\beta)$ for

$\mathbf{v}_t = (v_{1,t}, v_{2,t})'$, $\mathbf{w}_t^\mu = (w_{1,t}^\mu, w_{2,t}^\mu)'$, and $\mathbf{w}_t^\beta = (w_{1,t}^\beta, w_{2,t}^\beta)'$. Model (23)–(25) can be expressed in the usual DLM form of (4)–(5); see the supplementary material.

We applied the nonparametric CDF transformation from (8) and the default rounding operation. Considering the length of the dataset, we chose to use the Gibbs sampler (see the supplementary material) for offline posterior inference, with \mathbf{V} , \mathbf{W}_μ , \mathbf{W}_β assigned inverse-Wishart priors. Our run of the MCMC algorithm returned 10000 samples of our offline dataset’s final state ($T = 730$), which became the input for the particle filter of Algorithm 2 (along with posterior estimates of the covariance matrices). After running this algorithm sequentially through each time point in the online dataset, the final result was 10000 sequential paths of our smoothed states. Using these smoothed states, we also iterated one step ahead to obtain draws from the forecasting distribution of our data as outlined in Section 3.2.3.

We evaluate the forecasting performance by first reporting calibration. In Figure 4, we plot the sorted rPIT values of both series against standard uniform quantiles. For a calibrated forecast, we would expect these lines to closely follow the 45-degree line. Since the rPIT values are random quantities, some variation is natural. To showcase the inherent variability that might result from uniform samples, we drew 100 samples of size $n = 396$ from the standard uniform, and plot their sorted values against the uniform quantiles.

The particle filter forecasts are well-calibrated for the other OD time series. For the heroin OD series, the calibration shows slight signs of being non-uniform, although the deviations are minor. The histogram of the rPIT values (not shown here) shows a slightly inverse-U shape, which implies forecasts are overdispersed relative to the actual values. A closer investigation of the data shows that the online dataset showed considerably less variation than the offline dataset. However, the nonparametric CDF transformation used in the particle filter was estimated with only the offline data. This suggests a need to

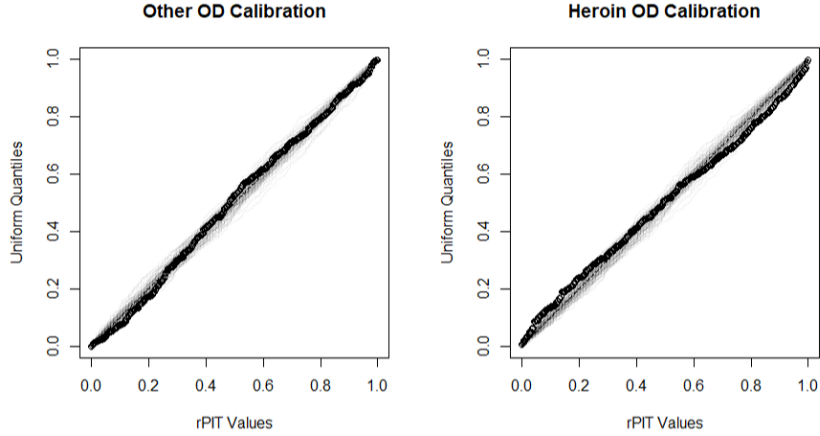


Figure 4: Randomized PIT plots from one-step-ahead particle filter forecasts for both overdose time series; dashed line is 45-degree line; lines with light shading show random uniform samples to give a sense of expected variability

occasionally re-calibrate the data-driven transformation when performing online inference.

Recall that this particle filter design is “optimal” in the sense of [Doucet et al. \(2000\)](#), achievable due to the analytic selection normal theory behind the warpDLM. We can see that this optimality results in a consistently high effective sample size (ESS), approximated using the normalized weights \tilde{w}_t at each time point: $ESS = 1 / \sum_{s=1}^S (\tilde{w}_t^{(s)})^2$. Crucially, the particle filter produces these effective samples quickly and in a manner that does not increase with the time index t . Figure 5 shows both the effective sample size across the time points of the particle filter as well as the number of seconds spent estimating the model at each time point (this analysis was performed on a laptop with an Intel Core i5-6200U CPU with 8 GB RAM). Most updates take around 13-14 seconds, which suggests that the particle filtering method could be used to model minute-by-minute streaming data. In all, the online algorithm of the warpDLM model shows promising results: it is applicable to multivariate count data, it produces calibrated forecasts for a real dataset, and the

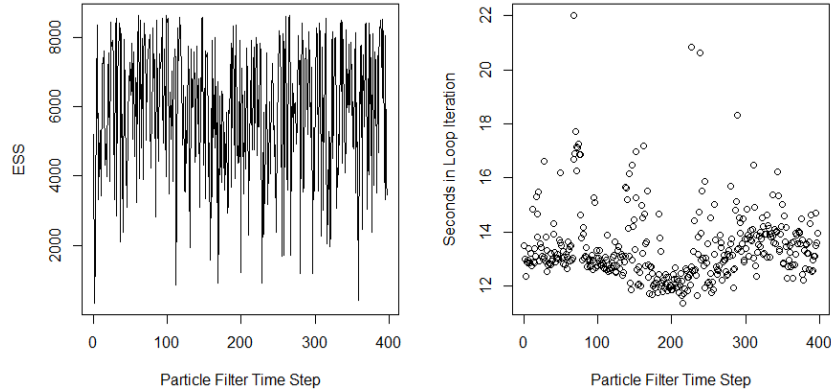


Figure 5: Left: Effective sample size across time points of the particle filter (10000 is maximum); Right: Seconds of computation per time loop of particle filter

computing scales sufficiently well for moderate- to high-frequency online analysis.

6 Conclusion

In this article, we have introduced a novel warpDLM methodology to model time series of counts. This framework adapts the familiar and flexible Gaussian linear state-space model for coherent usage in the discrete data case. It does so via a warping mechanism composed of transformation and rounding components that generalizes and extends a variety of discrete data approaches. Crucially, we showed that conjugate Bayesian inference is available for this model using the selection-normal distribution, leading to analytic filtering and smoothing recursions, a rare result in the count time series literature. This theory is directly impactful for algorithmic development, from Monte Carlo posterior sampling to an optimal particle filter for online learning. Using simulated data, have shown that the warpDLM framework offers better distributional forecasting than Bayesian competitors, particularly when the

count data exhibit multiple complexities such as zero-inflation and boundedness. Finally, we showcased how the warpDLM approach can perform online inference of multivariate count time series data. Because the warpDLM enables specification of both the discrete data support (via the rounding operator) and familiar DLMS or state space models—and is accompanied by the aforementioned efficient algorithms for offline and online inference—this modeling framework offers broad utility for count time series analysis.

The generality of the proposed warpDLM framework enables several useful extensions. Successful tools from (Gaussian) DLMS, such as scale-free variance modeling or discount factors, may be incorporated into the warpDLM framework. These specifications often result in t -distributed state updates and predictions, which may be linked to our results via the selection- t distribution. Similarly, other increases in modeling complexity can be accompanied by appropriate algorithmic advancements, such as sequential Monte Carlo methods that sample both the unknown parameters and the states concurrently (Chopin et al., 2012). Despite the inherent challenges in these more complex modeling and computing environments, the analytic and recursive updates derived for the warpDLM offer a promising pathway for efficient and perhaps optimal implementations.

References

- Aktekin, T., Polson, N., and Soyer, R. (2018). Sequential bayesian analysis of multivariate count data. *Bayesian Analysis*, 13(2).
- Andrieu, C., Doucet, A., and Holenstein, R. (2010). Particle markov chain monte carlo methods. *Journal of the Royal Statistical Society: Series B (Statistical Methodology)*, 72(3):269–342.

- Arellano-Valle, R. B., Branco, M. D., and Genton, M. G. (2006). A unified view on skewed distributions arising from selections. *Canadian Journal of Statistics*, 34(4):581–601.
- Berry, L. R. and West, M. (2019). Bayesian forecasting of many count-valued time series. *Journal of Business & Economic Statistics*, 38(4):872–887.
- Botev, Z. I. (2017). The normal law under linear restrictions: simulation and estimation via minimax tilting. *Journal of the Royal Statistical Society. Series B: Statistical Methodology*, 79(1):125–148.
- Box, G. E. P. and Cox, D. R. (1964). An analysis of transformations. *Journal of the Royal Statistical Society. Series B (Methodological)*, 26(2):211–252.
- Bradley, J. R., Holan, S. H., and Wikle, C. K. (2018). Computationally efficient multivariate spatio-temporal models for high-dimensional count-valued data (with discussion). *Bayesian Analysis*, 13(1).
- Campagnoli, P., Petrone, S., and Petris, G. (2009). *Dynamic Linear Models with R*. Springer New York.
- Canale, A. and Dunson, D. B. (2011). Bayesian kernel mixtures for counts. *Journal of the American Statistical Association*, 106(496):1528–1539.
- Canale, A. and Dunson, D. B. (2013). Nonparametric Bayes modelling of count processes. *Biometrika*, 100(4):801–816.
- Carter, C. K. and Kohn, R. (1994). On Gibbs sampling for state space models. *Biometrika*, 81(3):541–553.

- Chopin, N., Jacob, P. E., and Papaspiliopoulos, O. (2012). Smc2: an efficient algorithm for sequential analysis of state space models. *Journal of the Royal Statistical Society: Series B (Statistical Methodology)*, 75(3):397–426.
- Cox, D. R., Gudmundsson, G., Lindgren, G., Bondesson, L., Harsaae, E., Laake, P., Juselius, K., and Lauritzen, S. L. (1981). Statistical analysis of time series: Some recent developments [with discussion and reply]. *Scandinavian Journal of Statistics*, 8(2):93–115.
- Czado, C., Gneiting, T., and Held, L. (2009). Predictive model assessment for count data. *Biometrics*, 65(4):1254–1261.
- Doucet, A., Godsill, S., and Andrieu, C. (2000). On sequential monte carlo sampling methods for bayesian filtering. *Statistics and computing*, 10(3):197–208.
- Durbin, J. and Koopman, S. J. (2000). Time series analysis of non-gaussian observations based on state space models from both classical and bayesian perspectives. *Journal of the Royal Statistical Society: Series B (Statistical Methodology)*, 62(1):3–56.
- Ensor, K. B., Ray, B. K., and Charlton, S. J. (2014). Point source influence on observed extreme pollution levels in a monitoring network. *Atmospheric Environment*, 92:191–198.
- Fasano, A., Rebaudo, G., Durante, D., and Petrone, S. (2021). A closed-form filter for binary time series. *Statistics and Computing*, 31(4).
- Fokianos, K., Rahbek, A., and Tjøstheim, D. (2009). Poisson autoregression. *Journal of the American Statistical Association*, 104(488):1430–1439.
- Freeland, R. and McCabe, B. (2004). Forecasting discrete valued low count time series. *International Journal of Forecasting*, 20(3):427–434.

- Frühwirth-Schnatter, S. (1994). Data Augmentation and Dynamic Linear Models. *Journal of Time Series Analysis*, 15(2):183–202.
- Gamerman, D., dos Santos, T. R., and Franco, G. C. (2013). A non-gaussian family of state-space models with exact marginal likelihood. *Journal of Time Series Analysis*, 34(6):625–645.
- Helske, J. (2017). Kfas: Exponential family state space models in r. *Journal of Statistical Software*, 78(10).
- Jia, Y., Kechagias, S., Livsey, J., Lund, R., and Pipiras, V. (2021). Latent gaussian count time series. *Journal of the American Statistical Association*, page 1–11.
- Kalman, R. E. (1960). A new approach to linear filtering and prediction problems. *Transactions of the ASME—Journal of Basic Engineering*, 82(Series D):35–45.
- Kantas, N., Doucet, A., Singh, S. S., Maciejowski, J., and Chopin, N. (2015). On particle methods for parameter estimation in state-space models. *Statistical Science*, 30(3).
- Kolassa, S. (2016). Evaluating predictive count data distributions in retail sales forecasting. *International Journal of Forecasting*, 32(3):788–803.
- Kowal, D. R. (2021). Conjugate priors for count and rounded data regression. *arXiv preprint arXiv:2110.12316*.
- Kowal, D. R. and Canale, A. (2020). Simultaneous Transformation and Rounding (STAR) Models for Integer-Valued Data. *Electronic Journal of Statistics*.
- Kowal, D. R. and Wu, B. (2021). Semiparametric count data regression for self-reported mental health. *arXiv preprint arXiv:2106.09114*.

- Ledwina, T. (1994). Data-driven version of neyman’s smooth test of fit. *Journal of the American Statistical Association*, 89(427):1000–1005.
- Li, Z. R., Xie, E., Crawford, F. W., Warren, J. L., McConnell, K., Copple, J. T., Johnson, T., and Gonsalves, G. S. (2019). Suspected heroin-related overdoses incidents in Cincinnati, Ohio: A spatiotemporal analysis. *PLoS medicine*, 16(11):e1002956.
- Liboschik, T., Fried, R., Fokianos, K., and Probst, P. (2017). tscount: Analysis of Count Time Series.
- Prado, R. and West, M. (2010). *Time Series: Modeling, Computation, and Inference*. Chapman & Hall/CRC Texts in Statistical Science. Taylor & Francis.
- Siegfried, S. and Hothorn, T. (2020). Count transformation models. *Methods in Ecology and Evolution*, 11(7):818–827.
- West, M. and Harrison, J. (1997). *Bayesian Forecasting and Dynamic Models (2nd Ed.)*. Springer-Verlag, Berlin, Heidelberg.
- West, M., Harrison, P. J., and Migon, H. S. (1985). Dynamic generalized linear models and bayesian forecasting. *Journal of the American Statistical Association*, 80(389):73–83.